Biol. Cell (2015) **107,** 1–13 DOI: 10.1111/boc.201500003

Research article

Crosstalk of EGFR signalling with Notch and Hippo pathways to regulate cell specification, migration and proliferation in cockroach panoistic ovaries

Nashwa Elshaer*† and Maria-Dolors Piulachs*

*Institut de Biologia Evolutiva, CSIC-Universitat Pompeu Fabra, Barcelona 08003, Spain and †Permanent address: Department of Pest Control, Faculty of Agriculture, Zagazig University, Egypt

Background information. Epidermal growth factor receptor (EGFR) signalling is crucial for the regulation of multiple developmental processes. Its function in relation to insect oogenesis has been thoroughly studied in the fly *Drosophila melanogaster*, which possesses ovaries of the highly modified meroistic type. Conversely, studies in other insect species with different ovary types are scarce. We have studied EGFR functions in the oogenesis of the cockroach *Blattella germanica*, a phylogenetically basal insect with panoistic ovaries.

Results. In this cockroach, depletion of EGFR expression aborts oocyte maturation and prevents oviposition, as affects the distribution of F-actins in the follicular cells of the basal ovarian follicle, which triggers premature apoptosis. In the younger ovarian follicles within the ovariole, depletion of EGFR expression reduces the number of follicular cells, possibly because the Hippo pathway is altered; moreover, the concomitant reduction of Notch expression results in the absence of stalk. Finally, depletion of EGFR determines an increase in the number of germinal cells.

Conclusions. In the panoistic ovary of *B. germanica*, EGFR plays a role in the control of cell proliferation through interaction with Hippo and Notch pathways.

Additional supporting information may be found in the online version of this article at the publisher's web-site

Introduction

The epidermal growth factor receptor (EGFR) is a key regulator in fundamental functions of multiple development processes, being highly conserved in vertebrates and invertebrates (Stein and Staros, 2006), showing a high diversity of functions due to its five ligands (Spitz, Argos, Gurken, Vein and Keren) (Shilo, 2003, 2005). In the fruit fly *Drosophila melanogaster*, for example, EGFR acts as either an inhibitor or as an activator in all developmental stages, from embryo to adult, and in a great number of functions (cell proliferation, cell fate determination, patterning, apoptosis, etc.) (Shilo, 2003). During early oogenesis of this fly, the EGFR gene is expressed in the somatic cells (Sapir et al., 1998) encapsulating each oocyte with the corresponding nurse cells in the germarium prior to egg chamber formation (Goode

To whom correspondence should be addressed (email: mdolors.piulachs@ibe.upf-csic.es).
Key words: *Blattella germanica*, *Drosophila melanogaster*, Epidermal growth factor, Follicular cells, Insect reproduction.
Abbreviations: BgEGFR, EGFR mRNA of B. germanica; DAPI, 4′,6-diamidino-2-phenylindole; EGFR, epidermal growth factor receptor; MAPK, mitogen-activated protein kinase; NICD, Notch intracellular domain; qRT-PCR, quantitative real-time PCR.

et al., 1996). In mid-oogenesis, EGFR activates the follicular cells overlying the posterior pole of the egg chamber, thus inducing them to take a posterior fate (Gonzalez-Reyes et al., 1995; Roth et al., 1995). In late oogenesis, EGFR activates the dorsal follicular cells that overly close to the oocyte nucleus, inducing them to develop the egg appendages (Gonzalez-Reyes et al., 1995).

In insects there are three major ovary types, the panoistic and two meroistic types, the polytrophic and the telotrophic. In sharp contrast to the comprehensive data collected on *D. melanogaster* that possess meroistic polytrophic ovaries, the knowledge of the action of EGFR in oogenesis in other insect species, with less-modified ovarian types, is scarce. An exception to this observation is a study on the expression of EGFR in relation with oogenesis in the cricket *Gryllus bimaculatus* (Lynch et al., 2010). The ovaries of *G. bimaculatus* belong to the panoistic type, which is the least modified among insect ovaries. It is characterised by the absence of nurse cells accompanying the oocyte; moreover, in most species the oocyte nucleus keeps a central position without migrating to the anterior pole as occurs in the meroistic polytrophic type (Büning, 1994). In *G. bimaculatus*, EGFR mRNA was localised in the follicular cells surrounding the oocyte and the activation of EGF signalling pathway has been demonstrated in these cells by detecting mitogen-activated protein kinase (MAPK) activity (by anti-dpERK labelling, which strongly labels the cells overlaying the oocyte nucleus) (Lynch et al., 2010).

In our research, we have used the cockroach *Blattella germanica* as a model. It is a hemimetabolous species with panoistic ovaries. A typical feature of *B. germanica* oogenesis is that the basal oocyte is the only one to mature in the gonadotrophic cycle; the other ovarian follicles remain in the vitellarium to take up the basal position in following cycles, when development will be resumed (Herraiz et al., 2014; Irles et al., 2009; Irles and Piulachs, 2014). We have confirmed the presence and the activity of EGFR in the oocytes of *B. germanica*, spreading to the cytoplasm and to the nucleus. It is necessary for the proper development of the ovarian follicle, although its action is different depending on the follicle development stage and the nature of the cell line (germinal or somatic). Our study has established a clear relationship between EGFR signalling and the Notch and Hippo pathway, suggesting that EGFR plays a key role in controlling the correct proportion of germinal (oocytes) and somatic (follicular) cells.

Results

Expression and localisation of EGFR in *B. germanica* ovaries

The EGFR mRNA of *B. germanica* (BgEGFR) was extracted from ovarian tissues, then reverse transcribed, amplified, cloned and sequenced. BgEGFR has an ORF of 4890 bp encoding for a protein of 1452 amino acids, which is highly similar to other insect EGFR homologs.

Ovarian expression of BgEGFR was measured in sixth instar nymphs and adults, revealing that the expression is generally higher in nymph rather than adult ovaries. The highest levels were measured in the first day of the sixth nymphal instar and then tended to decrease smoothly and progressively as oocytes mature, reaching the lowest levels in 7-day-old females, just before oviposition occurs (Figure 1A).

A heterologous antibody against the *D. melanogaster* EGFR was used to localise the BgEGFR protein in the ovaries of *B. germanica*. In all stages studied, labelling for BgEGFR was detected in both somatic (follicular cells) and germ cells (oocytes) (Figure 1). At the end of the sixth nymphal instar, BgEGFR labelling in the basal oocyte appeared to be diffused throughout the cytoplasm, but with an increased signal close to the nuclear membrane (Figures 1B and 1D). At this age (8-day-old last instar nymphs), the same distribution of labelling, spread by the cytoplasm and more concentrated around the nucleus, was observed in all ovarian follicles within the ovariole (Figure 1D). However, in the germinal cells still located in the germarium and in the upper follicles from some ovarioles (Figures 1B and 1C), the EGFR labelling appeared as spots, also with an increase of the labelling around the nucleus. It is worth noting that labelling was less intense in the anterior and posterior poles of the oocytes (Figure 1D). At this age, the follicular cells showed a faint BgEGFR labelling, although a higher intensity was observed in the apical pole (Figure 1E). We used an antibody against dpERK to detect the activation of the EGF signalling cascade, and the labelling obtained for the activated MAPK coincided with that of BgEGFR (Figure S1). After the adult moult, BgEGFR labelling in basal follicles became

Figure 1 | EGFR in *B. germanica* ovaries

(**A**) Expression of BgEGFR in ovaries during the sixth nymphal instar and the first gonadotrophic cycle of adults. Data represent copies of BgEGFR mRNA per 1000 copies of actin-5c mRNA, and are expressed as the mean ± S.E.M. ($n = 4$ in sixth instar nymph, $n = 2$ in adults). (**B–E**) Immunolocalisation of EGFR protein (in green) in an ovariole taken from an 8-day-old sixth instar nymph; labelling can be observed in the oocyte cytoplasm, concentrated around the nucleus and within the oocyte nucleus. (**B**) Sub-basal ovarian follicle (sBOF), (**C**) germarium and (**D**) basal ovarian follicle. (**E**) Detail of the basal ovarian follicle showing the distribution of EGFR in follicular cells and where its location in the apical part. The apical (Ap) and basal (Ba) poles of the follicular cells are indicated. (**F**) Basal ovarian follicle from a 0-day-old adult female. EGFR labelling has a tendency to concentrate in the anterior–posterior poles. (**G**) Anterior pole of basal ovarian follicle of a 3-day-old adult female showing the labelling for EGFR concentrated in the anterior pole. (**H**) Detail of the basal ovarian follicle of a 3-day-old adult, showing the distribution of EGFR in the follicular cells. EGFR, green; F-actin, red; DNA, blue. The anterior pole of the ovarian follicles is towards the left. Scale bars: 50 μm.

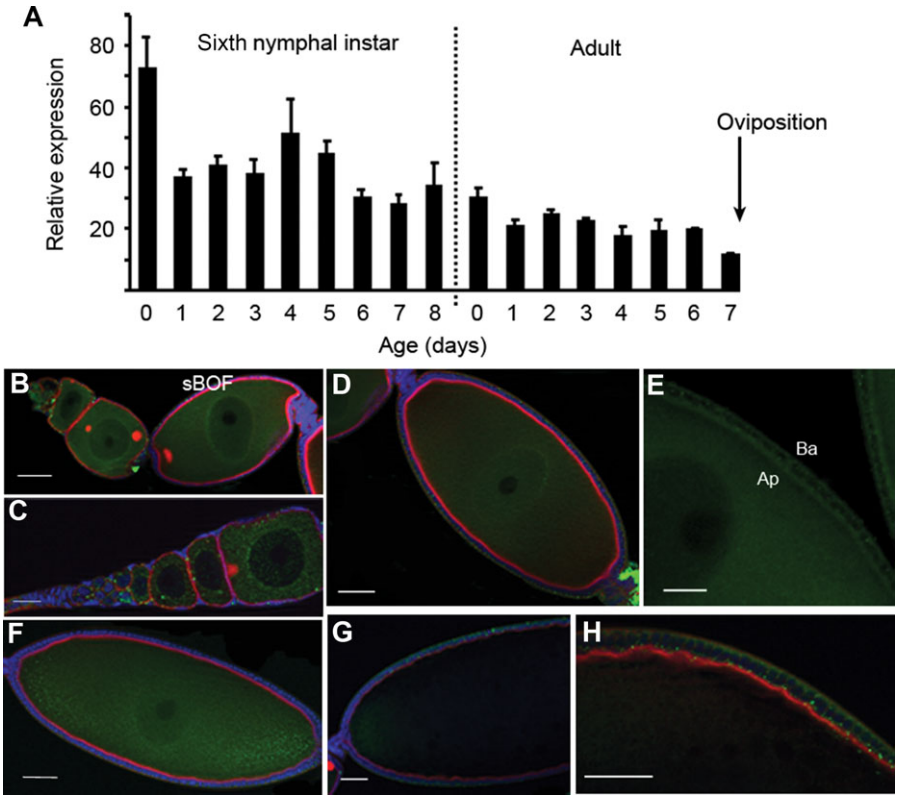

quite dynamic. In 0-day-old adult females, although labelling still distributed throughout the oocyte cytoplasm and the nucleus, it had a tendency to accumulate in the anterior and posterior poles of the basal oocyte (Figure 1F). In 3-day-old adult females, as the basal ovarian follicle matured, BgEGFR localisation was restricted to the anterior pole of the oocyte (Figure 1G), whereas the distribution in other oocytes of the ovariole remained similar to that observed in 8-day-old sixth instar nymphs. The distribution of BgEGFR labelling in the adult follicular cells was modified, appearing in a basolateral position (Figure 1H).

BgEGFR depletion impairs egg production and laying

BgEGFR functions related to oocyte development in *B. germanica* were studied using RNAi. A dose of 1 μg of dsBgEGFR was injected into 0-day-old sixth nymphal instar females ($n = 48$). The same dose

of an unspecific dsRNA (dsMock) was equivalently injected to control females ($n = 47$). The expression levels of BgEGFR were measured in ovaries at the last day (8-day-old) of the sixth nymphal instar (before the imaginal moult), in 3-day-old adult females (at the beginning of vitellogenesis) and in 5-day-old adult females (when the follicular cells change the cell cycle program by switching from mitosis to endocycle and when they exhibit patency). Levels of BgEGFR mRNA in ovaries of 8-day-old last instar nymphs were significantly lower (around 50%) than the controls (Figure 2A), a decrease that was maintained in 3-day-old adult females. Later, in 5-day-old adult females, levels of BgEGFR recovery, and even appeared to be overexpressed (Figure 2A). Despite this late recover, all BgEGFR-treated females failed to oviposit and did not form the ootheca, which led us to study the ovary of *B. germanica* in detail, in order to identify which processes were affected.

Different phenotypes in oocytes from BgEGFR-treated nymphs

Basal follicles from 8-day-old dsBgEGFR-treated sixth instar nymphs conserved the normal elliptical egg shape of untreated follicles (Figures 2B and 2D). BgEGFR labelling in the oocytes from dsBgEGFR-treated females was less intense with respect to controls and appeared to be concentrated in and around the nucleus (Figures 2D and S2), differing from the distribution in dsMock oocytes (Figures 2B and S2) where the labelling appeared throughout the ooplasm as well as the nucleus membrane. Additionally, labelling in the follicular cells was less intense in the apical pole (Figure 2F) than it was in the dsMock-treated nymphs (Figure 1E).

Although the basal follicle appeared to be unaffected in dsEGFR-treated sixth instar nymphs, all other ovarian follicles in the ovariole presented morphological differences with respect to those of dsMock-treated females. The sub-basal ovarian follicles were elongated, exhibiting a tightening in the central region, which gave them a dumbbell-like or hourglass-like shape (Figures 2H and 2J, arrowheads). The distribution and intensity of BgEGFR labelling (spread throughout the cytoplasm but concentrated in and around the nucleus) in these sub-basal follicles from dsEGFR-treated females (Figure 2E) was similar to that observed in the sub-basal follicles of dsMock-treated specimens (Figures 2C).

Moreover, in these sub-basal follicles from 8-day-old dsBgEGFR-treated sixth instar nymphs, the follicular epithelium showed a 68% reduction in follicular cell numbers in comparison with controls, and had similar cell numbers than sub-basal follicles from 0-day-old sixth instar nymphs. These cells have a large irregularly shaped nucleus (Figures 2J and 3B), and cannot cover the whole surface of the follicle.

The cytoskeleton in dsBgEGFR-treated ovarian follicles was notably affected. An increase of F-actins in the oocyte membrane at the anterior pole of basal (Figures 2D, arrow, and S2B) and sub-basal (Figure 2E, arrow) oocytes was observed. Moreover, the follicular cells of sub-basal follicles revealed an increase staining intensity of β-tubulin microfilaments (Figure 2J) that were randomly distributed and unable to maintain the connection between cells. This was in contrast to the situation observed in sub-basal follicles of dsMock-treated females (Figure 2I) which presented a regular distribution of microtubules between the cells. The reduced number of cells in the follicular epithelium also affected the stalk; in most dsBgEGFR-treated females there was no stalk between the sub-basal and basal oocytes and only a few follicular cells could eventually be observed in its place (Figures 2H and 4C).

After moulting to the adult stage, the BgEGFR depletion phenotype in the sub-basal follicles was maintained and expressed to an even greater extent (Figure S3). The hourglass-like shape phenotype in sub-basal ovarian follicles was more accentuated, while tumour-like structures also appeared in association (Figure S3C). The basal ovarian follicle is the only present in some females, whereas the rest of ovarian follicles in the ovariole had disappeared leaving only the *tunica propria* and germarium remnants (Figure S3D).

BgEGFR depletion affects Hippo pathway

The low number of cells in the sub-basal ovarian follicles of dsBgEGFR-treated females suggests that mitosis was impaired (Figures 3A and 3B). This was confirmed by labelling the mitotic figures in the basal and sub-basal ovarian follicles of dsBgEGFR- and dsMock-treated 8-day-old sixth instar nymphs with anti-PH3 and quantifying them (Figures 3D–3G). There was significantly ($P = 0.0001$) less mitoses

Figure 2 | Depletion of EGFR in ovarian follicles from 8-day-old sixth instar nymphs

(**A**) Expression levels of BgEGFR in ovaries from 8-day-old sixth instar nymphs (N6D8), 3-day-old (AdD3) and 5-day-old (AdD5) adult females treated with dsBgEGFR or dsMock. Data represent normalised values against controls (reference value = 1) and are expressed as the mean ± S.E.M. ($n = 3$), according to the Relative Expression Software Tool 2008. (**B**) Basal ovarian follicle and (**C**) young ovarian follicles from dsMock-treated nymphs, showing the immunolocation of EGFR. (**D**) Basal ovarian follicle and (**E**) sub-basal follicle from dsBgEGFR-treated nymphs. EGFR labelling is attenuated in the anterior and posterior poles of the oocyte, appearing within the nucleus; the arrow shows a greater concentration of F-actins in the anterior pole and the arrowheads the tightening produced by the concentration of F-actins. (**F**) Follicular cells from dsBgEGFR-treated nymph, showing attenuated EGFR labelling. (**G**) Ovariole from an 8-day-old dsMock-treated sixth instar nymph. (**H**) Ovariole from an 8-day-old dsBgEGFR-treated sixth instar nymph, showing the hourglass-like shape in the sub-basal ovarian follicle (sBOF). (**I** and **J**) Sub-basal ovarian follicle from 8-day-old dsMock-treated (**I**) and dsBgEGFR-treated (**J**) sixth instar nymphs showing the distribution of β-tubulin microfilaments (B-tub; green) that appear extended and disorganised. The arrowheads show the tightening region. In all images, the anterior pole of the ovarian follicles is on the left side. Scale bars: 50 μm (except in G = 1 mm).

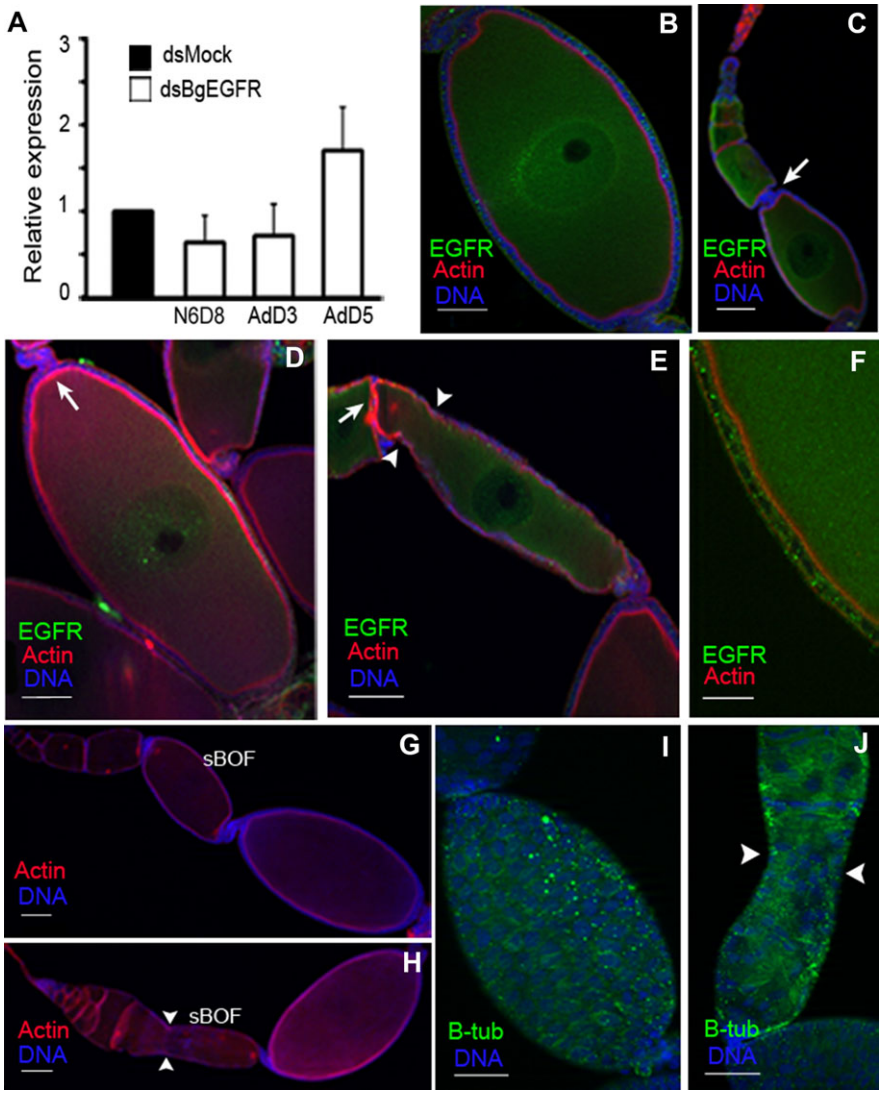

Figure 3 | BgEGFR depletion on follicular cells proliferation

(**A**, **B**) Sub-basal follicles from 8-day-old dsMock-treated (**A**) and dsBgEGFR-treated (**B**) sixth instar nymphs, showing the reduced number of follicular cells in dsEGFR-treated nymphs. (**C**) Number of mitoses labelled with PH3 in the follicular epithelium of basal and sub-basal ovarian follicles. Mitoses were quantified from pictures of basal and sub-basal ovarian follicles from different females ($n = 9$) that were labelled with PH3. Data are expressed as mean ± S.E.M. Asterisk indicates a significantly reduction ($P = 0.0001$) (**D–F**) ovarian follicles from an 8-day-old sixth instar nymph labelled with PH3 (pink) to show follicular cells in mitosis. (**D**) Basal follicle and (**E**) sub-basal follicle from 8-day-old dsMock-treated sixth instar nymph. (**F**) Basal follicle and (**G**) sub-basal follicle from 8-day-old dsBgEGFR-treated sixth instar nymph, with a lower rate of mitoses compared to the controls. The nuclei were stained with DAPI (grey). Scale bars: 50 μm. BOF, basal ovarian follicle; sBOF, sub-basal ovarian follicle. (**H**) Relative expression of different components in the Hippo pathway: BgHpo, BgMer and BgYki, in ovaries from 8-day old dsMock-treated and dsBgEGFR-treated sixth instar nymphs. BgHpo and BgYki were significantly reduced (P(H1) = 0 and 0.034, respectively). Data represent normalised values against the control (reference value = 1) and are expressed as the mean ± S.E.M. ($n = 3$), according to the Relative Expression Software Tool 2008.

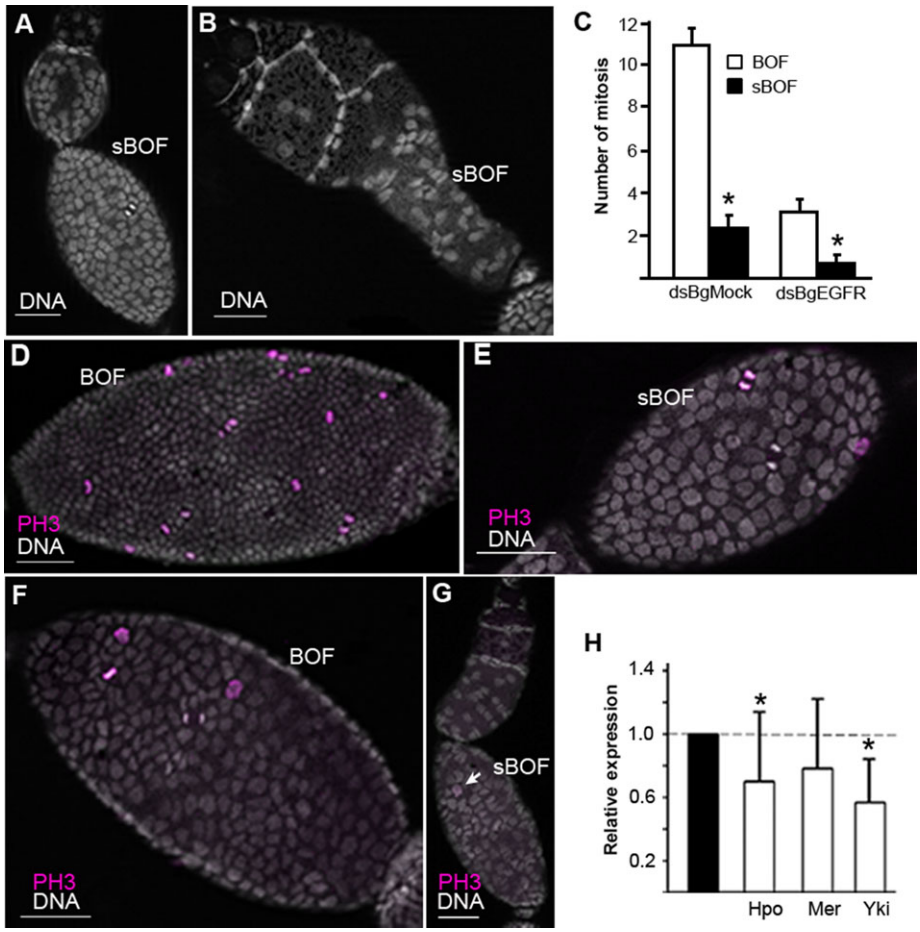

in both basal (72% reduction) and sub-basal (69% reduction) ovarian follicles from dsBgEGFR-treated females than in dsMock-treated females (Figures 3C). We wondered whether this decrease in cell division might be related with the Hippo pathway that controls follicular cell proliferation in *B. germanica* (Irles and Piulachs, 2014). We measured the expression of some of the components of this pathway in the ovary of 8-day-old dsBgEGFR-treated nymphs. Results indicated that the mRNA levels of Merlin (BgMer), an upstream component of the pathway, had a tendency to decrease. The expression of Hippo (BgHpo), a

Figure 4 | Effects of BgEGFR on germ cell proliferation

(**A**, **B**) Young oocytes and germarium from an 8-day-old sixth instar nymph; the nucleus from the germ cells were labelled with anti-Eya (green). (**A**) Germarium and vitellarium from a dsMock-treated nymph showing the ovarian follicles aligned within the ovariole. (**B**) Germarium and vitellarium from a dsBgEGFR-treated nymph, showing an excess of ovarian follicles. (**C**) The oocytes in dsBgEGFR-treated nymphs are neither organised nor encapsulated by a complete layer of follicular cells. (**D** and **E**) PH3 labelling (pink) in young oocytes and germarium, (**D**) germarium from a dsMock-treated nymph showing a single cell labelled for PH3 (arrow). (**E**) Germarium and vitellarium from a dsBgEGFR-treated nymph showing an increase in the number of PH3 labelled cells in the germarium (arrow). Scale bars: 50 μm (except in B = 1 mm).

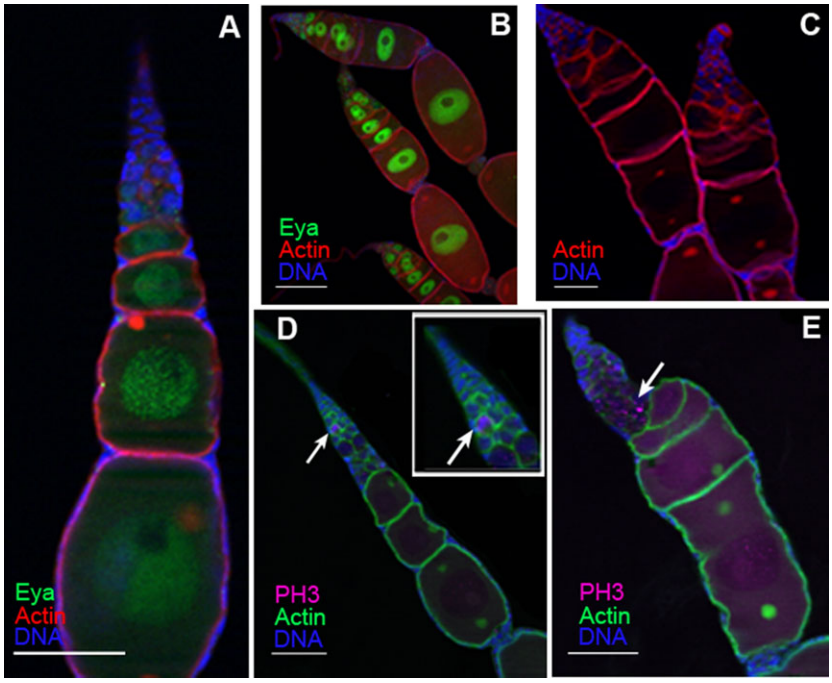

kinase in the core of the pathway, and Yorkie (BgYki), which is a downstream component, were significantly, although modestly, down-regulated (0.70- and 0.57-fold change, respectively) (Figure 3H). These results indicate that the Hippo pathway was affected by the depletion of BgEGFR.

Depletion of EGFR affects somatic and germinal cells, in younger ovarian follicles and in the germarium

The number of germ cells in the ovarioles of 8-day-old dsBgEGFR-treated sixth instar nymphs (Figure 4B) was higher than in controls (Figure 4A) and they overlapped in the region adjacent to the germarium (Figures 4B and 4C). This suggests that depletion of EGFR caused an increase in the rate of mitoses in the germinal stem cells that was confirmed by labelling mitoses with anti-PH3 antibody. Although in the germarium of most dsMock-treated females, only one germinal stem cell labelled with anti-PH3 was observed (Figure 4D), a large clusters of germ cells were labelled with anti-PH3 in the germarium of dsBgEGFR-treated females (Figure 4E, arrow), which points to an increase in cell division.

A reduced number of follicular cells were a consistent phenotype in all young oocytes from dsBgEGFR-treated females, which probably contributed to the structural collapse of the ovariole observed in these specimens. In both dsBgEGFR- and dsMock-treated females, the structure of the stalk remained between basal and sub-basal oocytes. However, a number of differences are observed between the sub-basal and the germarium. The follicular cells cannot cover the entirety of the young ovarian follicles in dsBgEGFR-treated females nor is there a sufficient amount to form the stalk between the

sub-basal and the following ovarian follicle (Figures 4C and S3B arrowhead). This contrasts with the observations for dsMock-treated females (Figure S3A) where two somatic cells are located between the ovarian follicles instead of the stalk (Figure S3A, arrowhead), reminiscent of the stalks that typically occur between the younger follicles in dsMock-treated females.

Given that the Notch pathway is required for the correct formation of stalk cells in *B. germanica* (Irles and Piulachs, 2014), we measured the expression of some components of this pathway in dsBgEGFR-treated sixth instar nymphs. The expression of BgN and its ligand BgDl tended to be down-regulated (60% and 25%, respectively), whereas that of BgSer, the other N ligand, tends to be up-regulated, as increased by around 40% (Figure 5A). The immunolocalisation of BgN, by using an anti-Notch intracellular domain (NICD) antibody in ovaries of 8-day-old dsBgEGFR-treated sixth instar nymphs, showed that the distribution of BgN labelling in the basal follicle was similar to that observed in the controls. However, there was a general decrease of BgN labelling in the sub-basal follicles of dsBgEGFR-treated nymphs (data not shown). BgDl protein in 8-day-old dsMock-treated nymphs was detected in all the oocytes and localised basolaterally in the follicular cells, except those of the anterior and posterior pole (Figures 5B and 5C). In dsBgEGFR-treated nymphs, the labelling for BgDl protein in basal ovarian follicles was reduced (Figure 5D), and the BgDl protein could be detected in the posterior pole of the sub-basal ovarian follicles (Figures 5E and 5E′ arrowhead). These results suggest that the Notch pathway responds to EGFR signalling, and the action of EGFR is different depending on the developmental stage of the ovarian follicle.

Figure 5 | BgEGFR and Notch pathway

(**A**) mRNA expression of different components of the Notch pathway in ovaries of 8-day-old sixth instar nymphs treated with dsBgEGFR. BgN had a tendency to decrease (P(H1) = 0.2), BgDl were not significantly affected, whereas BgSer had a tendency to be up-regulated (P(H1) = 0.195). Data represent normalised values against dsMock controls (reference value = 1) and are expressed as the mean ± S.E.M. (n = 3), according to the Relative Expression Software Tool 2008. (**B** and **C**) ovarian follicles from 8-day old dsMock-treated sixth instar nymphs. (**B**) Basal ovarian follicle showing the absence of BgDl labelling in the anterior (**B′**) and posterior (**B′**) poles, and also in the sub-basal ovarian follicle (**C**). (**D–E**) ovarian follicles of dsBgEGFR-treated specimens, showing less labelling for BgDl in basal follicles (**D**) and an irregular distribution in the sub-basal follicle (**E**), appearing labelling for BgDl in the posterior pole of the oocyte (arrowhead in **E′**). In all images, the anterior pole of the ovarian follicle is towards the top-left corner. BOF, basal ovarian follicle; sBOF, sub-basal ovarian follicle. Delta labelling, green; F-actin, red; DAPI, blue. Scale bars: 50 μm.

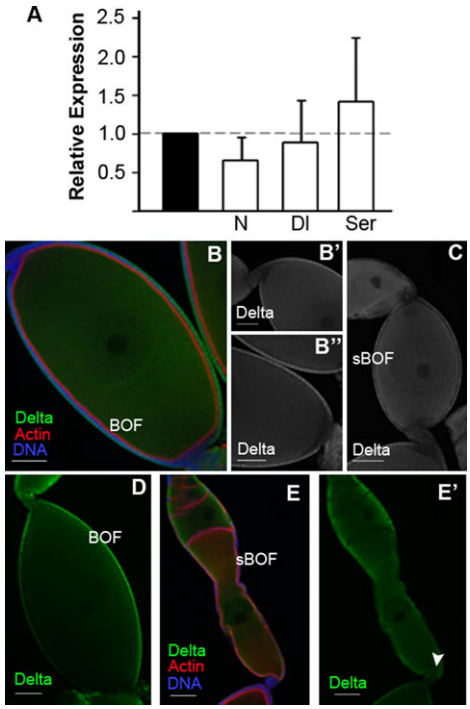

BgEGFR controls apoptosis in basal ovarian follicular cells

Although the oocytes from basal ovarian follicles in dsBgEGFR-treated females completed the chorion, as the sponge-like body is clearly visible in all of them, they were not oviposited. Only few of these oocytes reach the lateral oviduct remaining there until they were resorbed. Thus, we analysed the basal oocytes in adults at the end of the gonadotrophic cycle (7-day-old females), just before the oviposition time. In both dsBgEGFR- and dsMock-treated specimens, follicular cells of the basal ovarian follicles were binucleated (Figures 6A and 6C), and F-actins were mainly distributed adjacent to the cell membrane (Figures 6B and 6D). However, cell shape

Figure 6 | BgEGFR depletion on basal oocyte development Basal ovarian follicle from 7-day-old dsMock-treated (**A** and **B**) and dsBgEGFR-treated (**C** and **D**) adult females showing binucleated follicular cells. F-actins give a different shape to follicular cells in dsBgEGFR-treated females (**D**), compared with the hexagonal shape observed in dsMock-treated specimens (**B**). (**E** and **F**) Immunolocalisation of caspase-3 in follicular cells from the basal ovarian follicle of 7-day-old dsMock-treated (**E** and **E′**) and dsBgEGFR-treated adult females (**F** and **F′**), showing more cells labelled for caspase-3 in dsBgEGFR-treated follicles. DAPI, blue; F-actin, red; caspase-3 labelling, green. Scale bars: 50 μm.

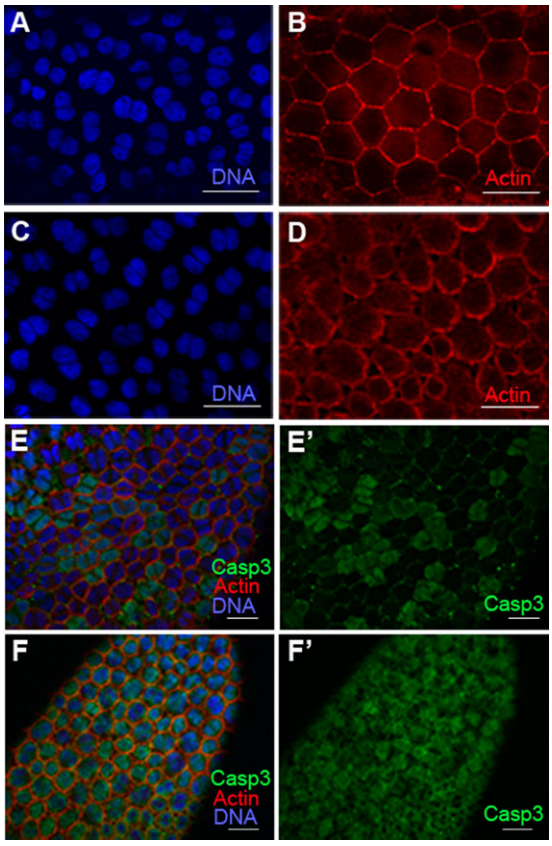

and size were affected by dsBgEGFR treatment, as follicular cells were of a non-uniform size and rounded (Figure 6D), thus not showing the hexagonal morphology of epithelial cells which is typical in the controls (Figure 6B).

The phenotype of these follicular cells suggested that they could be dying. To test this hypothesis, we used an anti-caspase-3 antibody to detect apoptotic cells. The nuclei of some follicular cells were labelled for caspase-3 in dsMock-treated specimens, the cells appearing grouped together in patches that were randomly distributed throughout the epithelium (Figures 6E and 6E′). By contrast, all follicular cells from basal follicles of dsBgEGFR-treated specimens revealed caspase-3 labelling in both the nuclei and the cytoplasm (Figures 6F and 6F′), which suggests that cell death occurred earlier in BgEGFR-depleted specimens than in controls.

Discussion

In recent years, thorough studies carried out into EGFR have shown that it acts as a key molecule for many multicellular organisms through its involvement in a wide variety of developmental processes, such as cell proliferation, differentiation and cell survival (Shilo, 2005). And related with that has also been intensively studied as a target gene in cancer therapies (Brand et al., 2013).

Studies in insects have revealed that EGFR is involved in different pathways of cell life. In the ovaries of *D. melanogaster*, EGFR is needed to specify the dorsal follicular cells that will form the egg appendages (Simakov et al., 2012) and to maintain the pool size of primordial germ stem cells (Matsuoka et al., 2013). In the honeybee *Apis mellifera*, EGFR signalling is involved in queen-worker caste differentiation (Kamakura, 2011) and induces reproductive capabilities in worker bees, as EGFR depletion determines that workers cannot activate the ovaries in a queenless environment (Formesyn et al., 2014).

We have shown that EGFR is also related with oogenesis in *B. germanica*, as its depletion prevents oviposition and ootheca formation. Localisation of BgEGFR protein is very dynamic; its distribution in the oocyte cytoplasm and around the nuclear membrane is modified with the age of the female. And by labelling dpERK we have shown that the EGF signalling pathway is active in the oocytes of *B. germanica*. Expression of EGFR was reported in oocytes and nurse cells of *D. melanogaster* (Kammermeyer and Wadsworth, 1987); given that translation was not assessed, expression was associated to maternal mRNAs destined to serve as functional mRNAs in embryogenesis. The occurrence of EGFR in the nucleus of somatic cells is nothing new as this localisation has been described in different cell lines or in cells from

different cancer types, always in relation to proliferative activity, functioning as a co-transcription factor that binds specific DNA sequences and activates genes involved in cell proliferation (Lin et al., 2001; Brand et al., 2011; Brand et al., 2013). The presence of BgEGFR in the nucleus of the oocyte from panoistic ovaries is probably related to the transcriptional activity preserved in the oocytes so they may provide all the materials required for the maturation of the oocyte itself and for the future embryo. This is not the case in *D. melanogaster*, where the oocyte nucleus is inactive and oocyte maturation depends on the nurse and follicular cells.

The role of BgEGFR in the ovarian follicles of *B. germanica* differs depending of the developmental stage. As mentioned before, in *B. germanica*, only the basal ovarian follicle in the ovariole can uptake vitellogenin and reach maturation in each gonadotrophic cycle. The morphology of the basal ovarian follicles appears to be unaffected by a depletion of BgEGFR expression as they complete its development and synthesise the chorion forming the sponge-like body at the end of the gonadotrophic cycle (Irles et al., 2009), indicating that the expression of EGFR in the follicular epithelium might not be related with the signalling of chorion synthesis. Differing to the EGFR signalling in the meroistic ovary of *D. melanogaster*, where EGFR is key for the correct positioning of egg appendages (Gonzalez-Reyes et al., 1997; Niepielko et al., 2014). Although these dsBgEGFR-treated females complete the chorion, these basal oocytes are not finally oviposited, probably due to the premature death of the follicular cells and to changes in actins distribution.

However, BgEGFR depletion deeply affects the structure of the sub-basal and more distal ovarian follicles, as they lose their ovoidal morphology and can even overlap each other. A possible cause of this phenotype could be related to changes in F-actins architecture, as they are highly disorganised in these young follicles. In sub-basal follicles, F-actins appear concentrated in the equatorial zone, tightening the area and given rise to these follicles an hourglass-shape. This phenotype is reminiscent of that observed in mouse oocytes after polymerising the actin microfilaments with the drug jasplakinolide (Calarco, 2005). Another consequence derived from BgEGFR depletion is a reduction in the number of follicular cells in young ovarian follicles that are in an insufficient amount to completely encapsulate the oocyte. A phenotype that has also been observed in other insect species, such as *D. melanogaster* where EGFR is involved in the regulation of cell migration (Goode et al., 1996), as well as in vertebrates, where a relationship between EGFR expression levels and oncogenic cell proliferation has been demonstrated (Brand et al., 2013; Berasain and Avila, 2014; Zhen et al., 2014). As follicular cell number was reduced, and the stalk cell precursors did not migrate, the stalk between the early ovarian follicles did not form properly, thus leading to overlapping of the sub-basal follicle and those that are leaving the germarium. Similar changes in the shape of early ovarian follicles have also been described in *G. bimaculatus* upon depleting EGF, the ligand of EGFR, and where the malformation was related to a defect in the anterior–posterior axis of the ovariole that affected the growth of the early ovarian follicles (Lynch et al., 2010).

Notch regulates the formation of the stalk in both panoistic (Irles and Piulachs, 2014) and meroistic ovaries (Lopez-Schier and St Johnston, 2001; Torres et al., 2003). Depletion of Notch activity results in a complete absence of the stalk connecting the ovarian follicles, an action that is mediated by the Hippo pathway (Irles and Piulachs, 2014) because BgHpo maintains BgN levels at an optimum for correct stalk formation. The functions of EGFR in relation to stalk formation in *B. germanica* herein reported seem to operate through other components of the Hippo pathway, as the reduced number of follicular cells is not explained by a reduced levels of BgHpo expression (Irles and Piulachs, 2014), but rather by the reduction of BgYki expression that occurs when BgEGFR is depleted. This kind of relationship has been described in the glial cells of *D. melanogaster* where EGFR stimulates the expression of Yki, thus maintaining the cell proliferation rate (Reddy and Irvine, 2013). In ovaries of dsBgEGFR-treated females, the low number of follicular cells showing mitosis contrasts with the over proliferation of germinal cells. A similar situation is observed with respect to the action of EGFR over primordial germ cell proliferation in *D. melanogaster*, where in this case, the receptor mediates the communication between the intermingled cells and the primordial germ cells in the developing ovary. The EGFR signalling that operates in the proliferation of primordial germ cells is

necessary for the survival of intermingled cells, which in turn send a feedback signal that inhibits further proliferation of primordial germ cells (Matsuoka et al., 2013). The hippo signalling mediates in the communications between germ cells and somatic cells and contributes to reach a correct proportion of both cell population (Sarikaya and Extavour, 2015). However, EGFR and Hippo are not the only ones that participate in maintaining the germ stem cells number. In this interplay also participates Notch signalling, as changes in the activation degree of Notch during the niche formation determines the number of cap cells in the germarium, and consequently the number of germ stem cells (Xie et al., 2008). In neural tissues of the worm *Caenorhabditis elegans* and the fly *D. melanogaster*, EGFR and Notch can have either agonistic or antagonistic functions in neural stem cells renewal, maintaining a balance between the different cell types (Aguirre et al., 2010). A similar mechanism can be envisaged in the ovary of *B. germanica*, acting in the germarium to control germ cell proliferation. Under normal conditions, a balance between the number of follicular cells and the number of oocytes produced in the germarium appears to be crucial; when depletion of EGFR reduces the quantity of follicular cells, they are on insufficient number to impede germ cell proliferation.

In summary, EGFR signalling in the ovary of *B. germanica* appears to play a central role by interacting with key pathways: the Notch pathway, controlling cell fate specification and cell migration, and the Hippo pathway, playing a fundamental role in the control of cell proliferation.

Material and methods

Cockroach colony and tissue sampling

Freshly ecdysed sixth instar nymphs or adult females of *B. germanica* were obtained from a colony maintained in the laboratory fed on Panlab dog chow and water *ad libitum*, and reared in the dark at 29 ± 1°C and 60%–70% relative humidity (Belles et al., 1987). 0-day-old adult females were maintained with males during all the first gonadotrophic cycle, and mating was confirmed at the end of the experiments by assessing the presence of spermatozoa in the spermatheca. All dissections and tissue sampling were carried out on carbon dioxide-anaesthetised specimens.

Cloning and sequencing

Sequence for EGFR of *B. germanica* (BgEGFR; Accession number: LN623701) was obtained from *B. germanica* ovarian mRNA library available in the laboratory. Sequence was confirmed by PCR amplification using ovarian cDNA as a template. The amplified fragments were cloned into the pSTBlue-1 vector (Novagen) and sequenced.

RNA extraction and reverse transcription to cDNA

All RNA extractions were performed using the GenElute Mammalian Total RNA kit (Sigma). RNA quantity and quality were estimated by spectrophotometric absorption at 260 nm/280 nm in a Nanodrop Spectrophotometer ND-1000® (Nano Drop Technologies, Wilmington, DE, USA). A sample of 400 ng of total RNA from each extraction was DNase treated (Promega) and reverse transcribed with Transcriptor First Strand cDNA Synthesis Kit (Roche). In all cases, the manufacturer protocols were followed.

Expression studies

Quantitative real-time PCR (qRT-PCR) was used to study BgEGFR expression. PCR primers used in qRT-PCR expression studies were designed using the Primer Express 2.0 software (Applied Biosystems), and are indicated in Supplementary Table S1. The efficiency of primers was first validated by constructing a standard curve through four serial dilutions of cDNA from ovaries. The actin-5c gene of *B. germanica* (Accession number AJ862721) was used as a reference (Irles et al., 2009; Herraiz et al., 2014). PCRs were made using the SYBR Green Supermix (BioRad) containing 200 nM of each specific primer, and were run in triplicate. Amplification reactions were carried out at 95°C for 2 min, and 40 cycles of 95°C for 15 s and 60°C for 30 s, using MyIQ Single Color RTPCR Detection System (Bio-Rad). qRT-PCR reactions were performed and analysed as previously described (Irles et al., 2009). Other *B. germanica* mRNA quantified in this work were Hippo (BgHpo, accession number: HF969251), Yorkie (BgYki, accession number: HF969253), Merlin (BgMer, accession number: HF969259), Notch (BgN, accession number: HF969255), Delta (BgDl, accession number: HF969256) and Serrate (BgSer, accession number: HG515375). The fold change expression was calculated using the REST-2008 program (Relative Expression Software Tool V 2.0.7; Corbett Research) (Pfaffl et al., 2002).

Depletion of EGFR mRNA by RNAi

To deplete BgEGFR expression, two dsRNAs (dsBgEGFR-1 and dsBgEGFR-2) were prepared encompassing a 516 bp and 283 bp in length. Preparation of the dsRNAs was performed as previously described (Ciudad et al., 2006). As control dsRNA (dsMock), was used a fragment (300 bp) of the sequence of *Autographa californica nucleopolyhedrovirus* (GenBank: K01149) (Lozano and Belles, 2011). Freshly emerged sixth instar nymphs were treated independently with 1 µg of each RNAi (dsBgEGFR-1, dsBgEGFR-2) injected into the abdomen in a volume of 1 µl of water-DEPC. The same dose and conditions were used with dsMock-treated females. As the same ovary phenotype was found using both dsBgEGFR-1 and dsBgEGFR-2, we will refer to the RNAi treatments as dsBgEGFR.

Immunofluorescence and cell staining

After dissection, ovaries were fixed immediately for 2 h with 4% paraformaldehyde in PBS, washed in PBT (PBS; 0.3% Triton-X100), treated with 50 µg/ml proteinase K for 2 min, washed for 2 min in 2 mg/ml glycine in PBT, washed for 10 min in

PBT and fixed again for 20 min with 4% paraformaldehyde in PBS. Then, three washed (10 min each) with PBT, and tissues were saturated for 1 h at RT in PBTBN (PBS; 0.1% Triton-X100, 0.5% BSA and 5% normal goat serum), and incubated overnight at 4°C in the primary antibody. The primary antibodies used were mouse anti-EGFR (15 µg/ml), anti-β-tubulin (1:50), anti-Notch (1:100), anti-Delta (1:100), the nucleus of the germ-line cells was labelled with anti-Eyes absent (Eya; 1:50) (Developmental Studies Hybridoma Bank, University of Iowa, Department of Biology, Iowa City, IA, USA). Rabbit anti-Phospho-Histone 3 (PH3) (1:250) anti-Caspase-3 (1:250) (Cell Signaling Technology) were used to label mitotic active cells and apoptotic cells respectively. Mouse anti-dpERK (1:50) (Sigma) was used to detect activated MAPK. Samples were washed with PBTBN three times and incubated for 2 h with Alexa-Fluor 647 conjugated goat anti-mouse IgG secondary antibody or Alexa-Fluor 647 conjugated donkey anti-rabbit IgG (Molecular Probes) both diluted 1:400 in PBTBN. For F-actin visualisation, ovaries were incubated for 20 min in 1 µg/ml phalloidin-TRITC (Sigma). Ovarioles were mounted in UltraCruz™ Mounting Medium (Santa Cruz Biotechnology®, Inc.), which contains 4′,6-diamidino-2-phenylindole (DAPI) for DNA staining. Samples were observed by epifluorescence microscopy using a Zeiss AxioImager.Z1 microscope (Apotome) (Carl Zeiss MicroImaging).

Statistics

The data are expressed as means ± standard error of the mean (S.E.M.). Statistical analyses between groups were made by ANOVA One way, with Tukey–Kramer multiple comparison test. Comparisons between treatment and control groups were made using the Pair-Wise Fixed Reallocation Randomization Test (which makes no assumptions about distributions) (Pfaffl et al., 2002), employing REST 2008 v. 2.0.7 software (Corbett Research).

Author contribution

N.E. performed the experiments. N.E. and M.D.P. analysed the data and wrote the article. M.D.P. conceived and designed the experiments and obtained the funding.

Funding

Support for this research was provided by the Spanish Ministry of Science and Innovation [Grant. BFU2011-22404], and from the Secretaria d'Universitats i Recerca del Departament d'Economia i Coneixement de la Generalitat de Catalunya [2014 SGR 619]. N.E. received a pre-doctoral research grant (JAE-Pre) from the CSIC, and The European Social Fund (ESF).

Acknowledgements

We are grateful to Prof. Xavier Belles for helpful scientific discussions and critical comments on the manuscript. The technical help of Elena Navas is also acknowledged.

Conflict of interest statement

The authors have declared no conflict of interest.

References

Aguirre, A., Rubio, M.E. and Gallo, V. (2010) Notch and EGFR pathway interaction regulates neural stem cell number and self-renewal. Nature **467**, 323–327

Belles, X., Casas, J., Messeguer, A. and Piulachs, M.D. (1987) In vitro biosynthesis of JH III by the corpora allata of adult females of *Blattella germanica* (L). Insect Biochem. Mol. Biol. **17**, 1007–1010

Berasain, C. and Avila, M.A. (2014) The EGFR signalling system in the liver: from hepatoprotection to hepatocarcinogenesis. J. Gastroenterol. **49**, 9–23

Brand, T.M., Iida, M., Li, C. and Wheeler, D.L. (2011) The nuclear epidermal growth factor receptor signaling network and its role in cancer. Discov. Med. **12**, 419–432

Brand, T.M., Iida, M., Luthar, N., Starr, M.M., Huppert, E.J. and Wheeler, D.L. (2013) Nuclear EGFR as a molecular target in cancer. Radiother. Oncol. **108**, 370–377

Büning, J. (1994) The Insect Ovary. London, Uk: Chapman & Hall.

Calarco, P.G. (2005) The role of microfilaments in early meiotic maturation of mouse oocytes. Microsc. Microanal. **11**, 146–153

Ciudad, L., Piulachs, M.D. and Belles, X. (2006) Systemic RNAi of the cockroach vitellogenin receptor results in a phenotype similar to that of the *Drosophila* yolkless mutant. FEBS J. **273**, 325–335.

Formesyn, E.M., Cardoen, D., Ernst, U.R., Danneels, E.L., VanVaerenbergh, M., DeKoker, D., Verleyen, P., Wenseleers, T., Schoofs, L. and deGraaf, D.C. (2014) Reproduction of honeybee workers is regulated by epidermal growth factor receptor signaling. Gen. Comp. Endocrinol. **197**, 1–4

Gonzalez-Reyes, A., Elliott, H. and St Johnston, D. (1995) Polarization of both major body axes in *Drosophila* by gurken-torpedo signalling. Nature **375**, 654–658

Gonzalez-Reyes, A., Elliott, H. and St Johnston, D. (1997) Oocyte determination and the origin of polarity in *Drosophila*: the role of the spindle genes. Development **124**, 4927–4937

Goode, S., Morgan, M., Liang, Y.P. and Mahowald, A.P. (1996) Brainiac encodes a novel, putative secreted protein that cooperates with Grk TGF alpha in the genesis of the follicular epithelium. Dev. Biol. **178**, 35–50

Herraiz, A., Belles, X. and Piulachs, M.D. (2014) Chorion formation in panoistic ovaries requires windei and trimethylation of histone 3 lysine 9. Exp. Cell Res. **320**, 46–53

Irles, P., Belles, X. and Piulachs, M.D. (2009) Identifying genes related to choriogenesis in insect panoistic ovaries by Suppression Subtractive Hybridization. BMC Genomics **10**, 206

Irles, P. and Piulachs, M.D. (2014) Unlike in *Drosophila* Meroistic Ovaries, Hippo Represses Notch in *Blattella germanica* Panoistic Ovaries, Triggering the Mitosis-Endocycle Switch in the Follicular Cells. PloS One **9**, e113850

Kamakura, M. (2011) Royalactin induces queen differentiation in honeybees. Nature **473**, 478–483

Kammermeyer, K.L. and Wadsworth, S.C. (1987) Expression of *Drosophila* epidermal growth factor receptor homologue in mitotic cell populations. Development **100**, 201–210

Lin, S.Y., Makino, K., Xia, W., Matin, A., Wen, Y., Kwong, K.Y., Bourguignon, L. and Hung, M.C. (2001) Nuclear localization of EGF receptor and its potential new role as a transcription factor. Nat. Cell Biol. **3**, 802–808

Lopez-Schier, H. and St Johnston, D. (2001) Delta signaling from the germ line controls the proliferation and differentiation of the somatic follicle cells during *Drosophila* oogenesis. Genes Dev. **15**, 1393–1405

Lozano, J. and Belles, X. (2011) Conserved repressive function of Kruppel homolog 1 on insect metamorphosis in hemimetabolous and holometabolous species. Sci. Rep. **1**, 163

Lynch, J.A., Peel, A.D., Drechsler, A., Averof, M. and Roth, S. (2010) EGF signaling and the origin of axial polarity among the insects. Curr. Biol. **20**, 1042–1047

Matsuoka, S., Hiromi, Y. and Asaoka, M. (2013) Egfr signaling controls the size of the stem cell precursor pool in the *Drosophila* ovary. Mech. Dev. **130**, 241–253

Niepielko, M.G., Marmion, R.A., Kim, K., Luor, D., Ray, C. and Yakoby, N. (2014) Chorion patterning: a window into gene regulation and *Drosophila* species' relatedness. Mol. Biol. Evol. **31**, 154–164

Reddy, B.V. and Irvine, K.D. (2013) Regulation of Hippo signaling by EGFR-MAPK signaling through Ajuba family proteins. Dev. Cell **24**, 459–471

Roth, S., Neuman-Silberberg, F.S., Barcelo, G. and Schupbach, T. (1995) Cornichon and the EGF receptor signaling process are necessary for both anterior-posterior and dorsal-ventral pattern formation in *Drosophila*. Cell **81**, 967–978

Saqrikaya, D.P. and Extavour, C.G. (2015) The Hippo pathway regulates homeostatic growth of stem cell niche precursors in the *Drosophila* ovary. PLoS Genet **11**(**2**): e1004962. doi:10.1371/journal.pgen.1004962

Sapir, A., Schweitzer, R. and Shilo, B.Z. (1998) Sequential activation of the EGF receptor pathway during *Drosophila* oogenesis establishes the dorsoventral axis. Development **125**, 191–200

Shilo, B.Z. (2003) Signaling by the *Drosophila* epidermal growth factor receptor pathway during development. Exp. Cell Res. **284**, 140–149

Shilo, B.Z. (2005) Regulating the dynamics of EGF receptor signaling in space and time. Development **132**, 4017–4027

Simakov, D.S., Cheung, L.S., Pismen, L.M. and Shvartsman, S.Y. (2012) EGFR-dependent network interactions that pattern *Drosophila* eggshell appendages. Development **139**, 2814–2820

Stein, R.A. and Staros, J.V. (2006) Insights into the evolution of the ErbB receptor family and their ligands from sequence analysis. BMC Evol. Biol. **6**, 79.

Torres, I.L., Lopez-Schier, H. and St Johnston, D. (2003) A Notch/Delta-dependent relay mechanism establishes anterior-posterior polarity in *Drosophila*. Dev. Cell **5**, 547–558

Zhen, Y., Guanghui, L. and Xiefu, Z. (2014) Knockdown of EGFR inhibits growth and invasion of gastric cancer cells. Cancer Gene Ther. **21**, 491–497

Xie, T., Song, X., Jin, Z., Pan, L., Weng, C., Chen, S. and Zhang, N. (2008) Interactions between stem cells and their niche in the *Drosophila* ovary. Cold Spring Harb. Symp. Quant. Biol. **73**, 39–47

Received: 7 January 2015; Accepted: 17 April 2015; Accepted article online: 23 April 2015

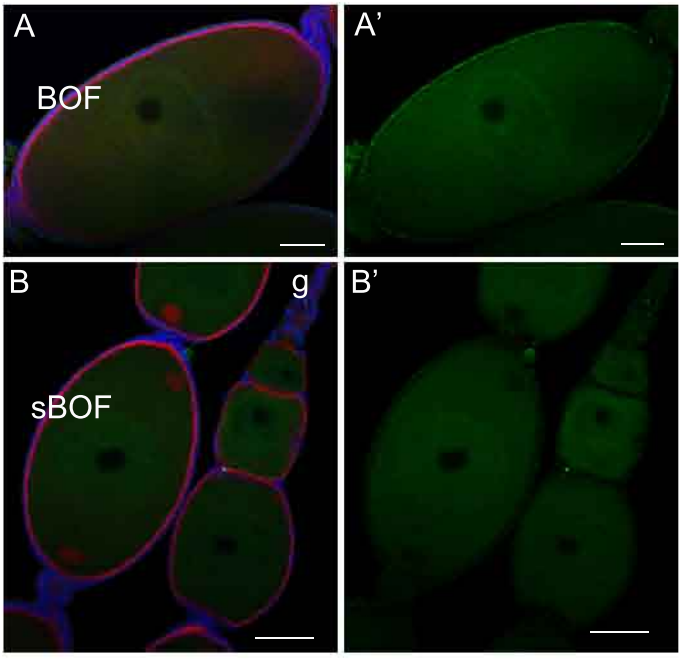

Figure S1: Detection of activated MAPK in sub-basal ovarian follicles from 8-day-old sixth instar nymphs. A mouse anti-dpERK antibody was used to label activated MAPK,(green) in basal (A, A') and sub-basal (B, B') ovarian follicles. BOF: basal ovarian follicle; sBOF: sub-basal ovarian follicle; g: germarium. F-actins (red) and DAPI (blue). Scale bars: 50 µm

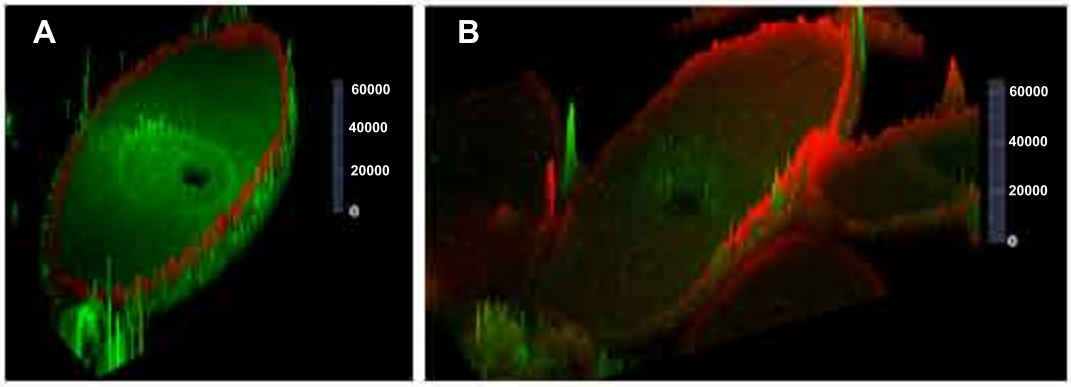

Figure S2: Intensity of EGFR labelling in a basal ovarian follicle from an 8-day-old dsMock-treated (A) and dsBgEGFR-treated (B) sixth instar nymphs. The signal intensity of the different fluorophores is shown using the option 2.5D of the Zen 2012 blue edition software from Zeiss. EGFR in green, F-actins in red.

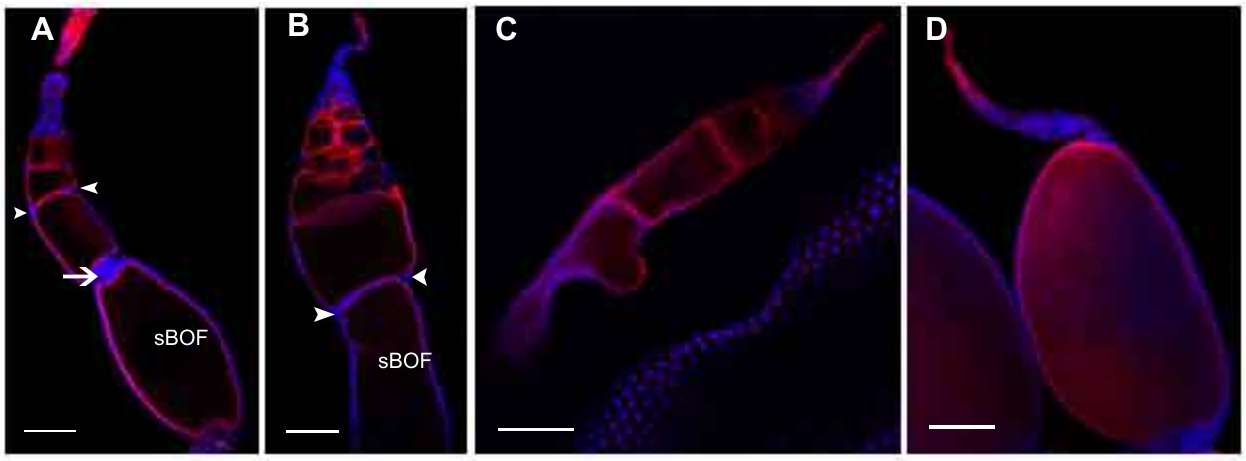

Figure S3: Depletion of BgEGFR on the stalk formation and in younger ovarian follicles. (A) Ovariole from an 8-day-old dsMock-treated sixth instar nymph, showing the correct stalk between the sub-basal ovarian follicle (sBOF) and the younger adjacent follicle (arrow). Between the rest of younger follicles, the stalks are not still formed, there are only two precursor cells that will be differentiated to form the stalk (arrowhead). (B) Ovariole from an 8-day-old dsBgEGFR-treated sixth instar nymph, showing the absence of the stalk between the sub-basal follicle (sBOF) and the younger adjacent follicle, only the precursor cells (arrowhead) can be detected between them. (C) Sub-basal ovarian follicle from a 5-day-old dsBgEGFR-treated adult, showing an accentuated hourglass-like phenotype with the oocyte that has broken the follicular epithelium. (D) Exceptionally, the dsBgEGFR treatment determines the loss of all ovarian follicles in the ovariole except the basal one that appeared connected to the rest of the germarium. F-actins: red, and DAPI: blue.Scale bars: 50 μm, except in (D) that is 100 μm.

Table S1: **Primer sequence used for qRT-PCR and RNAi experiments.** The accession numbers of studied sequences are indicated. F: Primer forward. R: Primer reverse. BgActin-5c was used as housekeeping gene in the expression studies.

	Accession number	**Primer name**		**Primer sequence**	**Amplicon length (bp)**
1	LN623701	BgEGFR-RT	F R	5' GAGTACAAAGCAGCAGGAG 3' 5' CCAACATCGGATATTCACTCAC 3'	76
2	LN623701	BgEGFR-RNAi1	F R	5' GAACACTGACCTGTGGATTGT 3' 5' TTGCTGATGAGTTTGCCAAG 3'	516
3	LN623701	BgEGFR-RNAi2	F R	5' GAATCCCCAACACCTCAGAA 3' 5' CTTACCAGTAGATGAAGATG 3'	283
4	HF969251	BgHpo-RT	F R	5' GACATTTGGAGCCTTGGCAT 3' 5' AGGTTTCCCTTCAGCCATTTC 3'	51
5	HF969253	BgYki-RT	F R	5' TCCCTACCACACACACCAGA 3' 5' GACCATCCAATGTTGCCATA 3'	103
6	HF969259	BgMer-RT	F R	5' CCGAAGCAGAACAGGAAATC 3' 5' CTGCTTCCCTTGTCTTACGC 3'	93
7	LN623700	BgCic-RT	F R	5' AACCCGCAAGGTTGTCAGT 3' 5' ACTCTGCTGCTCAAGCACAA 3'	150
8	HF969255	BgN-RT	F R	5' GCTAAGAGGCTGTTGGATGC 3' 5' TGCCAGTGTTGTCCTGAGAG 3'	55
9	HF969256	BgDl-RT	F R	5' CCACTACAAGTGTTCGCCAA 3' 5' TACCTCTCGCATTCGTCACA 3'	180
10	HG515375	BgSer-RT	F R	5' TCCTCTTGGCAGTGCATTTG 3' 5' CTTGATCACAGAGGATGCCG 3'	87
11	AJ862721	BgActin5c	F R	5' AGCTTCCTGATGGTCAGGTGA 3' 5' ACCATGTACCCTGGAATTGCCGACA 3'	213